Journal of
Materials Chemistry C

Accepted Manuscript

This article can be cited before page numbers have been issued, to do this please use: M. Nakashima, K. Iizuka, M. Karasawa, K. Ishii and Y. Kubo, *J. Mater. Chem. C*, 2018, DOI: 10.1039/C8TC00944A.

ROYAL SOCIETY OF CHEMISTRY

rsc.li/materials-c

View Article Online
DOI: 10.1039/C8TC00944A

Selenium-containing BODIPY dyes as photosensitizers for triplet-triplet annihilation upconversion

Mika Nakashima,[a] Keita Iizuka,[a] Masanobu Karasawa,[b] Kazuyuki Ishii[b] and Yuji Kubo*[a]

[a]*Department of Applied Chemistry for Environment, Graduate School of Urban Environmental Sciences, Tokyo Metropolitan University, 1-1 Minami-ohsawa, Hachioji, Tokyo 192-0397, Japan. *E-mail; yujik@tmu.ac.jp*
[b]*Institute of Industrial Science, The University of Tokyo, 4-6-1 Komaba, Meguro-ku, Tokyo, Japan*

Abstract: In this study, two new selenium-containing BODIPY dyes were synthesized as photosensitizers for triplet-triplet annihilation upconversion (TTA-UC). Bis(phenylselanyl)-BODIPY **1** absorbed visible light at 518 nm (ε_{max} = 7.84 × 10^4 cm^{-1} M^{-1}) and exhibited fluorescence at 594 nm with a low fluorescence quantum yield (Φ_F) of 0.03. The low Φ_F value was ascribed to heavy atom effects. When a TTA-UC system comprised of **1** and triplet acceptor perylene was set up, a purplish white emission was observed with a significant anti-Stokes shift of 77 nm and high UC quantum yield (Φ'_{UC}) of 17% in CH_2Cl_2. Notably, the intramolecular charge transfer of **1** enabled us to tune the emission color of the TTA-UC system. On the other hand, the use of selenophene derivative **2** as a sensitizer instead of **1** led to a decrease in the UC efficiency. The relationship between structure and sensitizer properties in the TTA-UC system is discussed herein.

Introduction

Triplet-triplet annihilation upconversion (TTA-UC) has garnered considerable interest because of its ability to harvest photoexcitation energy.[1-6] Its amenability with low power and incoherent photo excitation, such as by sunlight, allows for practical applications in the fields of lighting and photovoltaic devices[7, 8] as well as bioimaging.[9-11] Typical TTA-UC systems consist of a well-tailored sensitizer (S) and emitter (annihilator) (E). Under light illumination, the first singlet excited state of S is (^{1}S*), which is followed by intersystem crossing (ISC) to the triplet state (^{3}S*). In addition, triplet-triplet energy transfer (TTET) then occurs between the sensitizer and annihilator to enrich ^{3}E* species. Subsequently, triplet-triplet annihilation of two emitter triplets leads to the production of one emitter in the singlet state (^{1}E*). Given the synthetic diversity of organic dyes, new dyes applicable to TTA-UC constitute an intriguing research target. In this context, we focused on organic sensitizers due to their easier molecular design as compared to annihilators. Because efficient ISC is critical for sensitizers,[12] heavy atoms such as rare metals (Pt, Ru) and halogens (I, Br) have been employed in most sensitizers. Currently, effective triplet formation based on efficient ISC and long-lived triplet excited states have been explored for new design concepts, such as spin-orbital charge transfer intersystem crossing[13, 14] and radical-enhanced intersystem crossing[15] in addition to thermally activated delayed fluorescence,[16] leading to preparation of heavy metal-free sensitizers.

4,4-Difluoro-4-bora-3a,4a-diaza-*s*-indacene (BODIPY)-based dyes,[17-19] exhibit outstanding photophysical properties such as high molar extinction coefficients (ε), fluorescence quantum yields and photostabilities, which has led to their use in numerous applications.[20-30] Although BODIPY chromophore in itself is not a suitable triplet sensitizer, versatile derivatization of the BODIPY chromophore enables one to tune the photophysical properties.[31] 2,6-Diiode-BODIPYs are well-known triplet photosensitizers, wherein the introduction of iodide directly onto the dye skeleton results in a heavy atom effect and enhances the ISC process.[21] Considerable efforts have been put

View Article Online
DOI: 10.1039/C8TC00944A

forth to prepare various derivatives[32] and congeners[33] to date. Among them, **I_2-BODIPY** (Fig. 1) has been thoroughly investigated as a sensitizer for TTA-UC systems.[34, 35] In this context, **I_2-BODIPY** covalently connected by perylene was prepared although such a dyad showed no TTA-UC behavior.[36] It has also been pointed out that the introduction of iodide onto the chromophore leads to photo-induced cytotoxity.[37] Accordingly, exploration of new BODIPY-based triplet sensitizers is worthwhile because the facile modification of BODIPY can facilitate the preparation of efficient sensitizers with strong light harvesting abilities. With this strategy in mind, organoselenium compounds attracted our attentions. The relatively low toxicity has motivated chemists to prepare a number of selenium-containing compounds for application to electroconducting materials and catalysts.[38] Their pharmacological properties,[39] coupled with the low oxidation potentials have been used to sense reactive oxygen species, as well as biologically important thiols.[40, 41] In addition, redox-responsive probes based on selenium-containing fluorescent dyes have been reported.[42, 43] Given the versatile derivatization of BODIPYs, the combination of the "heavy atom effect" of selenium and the photophysical properties of the BODIPY chromophore may facilitate the production of an efficient photosensitizer for TTA-UC.

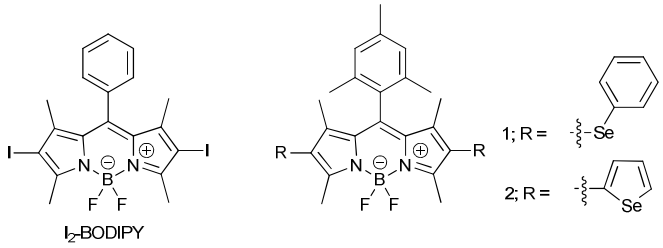

Fig. 1 Chemical structures of BODIPY dyes.

Here, bis(phenylselanyl)- and diselenopheno-BODIPY dyes **1** and **2** were synthesized and investigated as sensitizers for UC systems with perylene[44] as a triplet acceptor. Perylene was employed in this study due to the high fluorescence quantum yield and lower triplet energy than the sensitizer as required for a triplet acceptor in TTA-UC. Subsequently, when a TTA-UC system comprised of **1** and perylene was set up, an orange-to-purplish white UC emission was observed with a large anti-Stokes shift of 77 nm and high UC quantum yield (Φ'_{UC}) of 17% in CH_2Cl_2. To our knowledge, this is the first demonstration that a selenium-containing π-conjugated system can serve as a photosensitizer for applications in TTA-UC systems.

Experimental section

General

NMR spectra were taken by a Bruker Avance 500 (^{1}H: 500 MHz, ^{13}C: 126 MHz) spectrometer. In ^{1}H and ^{13}C NMR measurements, chemical shifts (δ) are reported downfield from the initial standard Me_4Si. Fast atom bombardment (FAB) mass spectra were obtained on a JEOL JMS-700 spectrometer where *m*-nitrobenzylalcohol was used as a matrix. The absorption and fluorescence spectra were measured using a Shimadzu UV-3600 and a JASCO FP-6500 spectrophotometers, respectively. Elemental analyses were performed on an Exeter Analytical, Inc. CE-440F Elemental Analyzer. Fluorescence lifetimes were determined by Hamamatsu photonics Quantaurus-Tau C11367-21.

View Article Online
DOI: 10.1039/C8TC00944A

Materials

Unless otherwise indicated, the reagents used for the synthesis were commercially available and used as supplied. 8-Mesityl-1.3,5,7-tetramethyl-4,4-difluoro-4-bora-3a,4a-diaza-s-indavene **3**,[45] 2,6-Diiodo-4,4-difluoro-1,3,5,7-tetramethyl-8-mesityl-4-bora-3a,4a-diaza-*s*-indacene **4**[46] and 4,4,5,5-tetramethyl-2-(selenophen-2-yl)-1,3,2-dioxaborolane[47] were prepared according to previously reported methods, respectively.

4,4'-Difluoro-1,3,5,7-tetramethyl-8-mesityl -2,6-bis(phenylselanyl)-4-bora-3a,4a-diaza-*s*-indacene 1

To a solution of **3** (0. 203 g, 0.554mmol) in dry CH_2Cl_2 (21 mL) was added PhSeCl (0. 210 g, 1.10 mmol). The reaction mixture was stirred at room temperature for 1.5 h, during which PhSeCl (0. 0209 g, 0.109 mmol) was added as a second portion. After removal of solvent, the residue was chromatographed on silica gel (Wakogel C-300) using a gradient eluent benzene in hexane (20 − 50%) and reprecipitated with CH_2Cl_2 / MeOH system to afford 0.317 g of **1** as a red solid in 85% yield. ^{1}H NMR (500 MHz, $CDCl_3$) δ (ppm) : 7.09 – 7.20 (m, 10H), 6.96 (s, 2H), 2.68 (s, 6H), 2.32 (s, 3H), 2.10 (s, 6H), 1.51 (s, 6H) ; ^{13}C NMR (126 MHz) 159.7, 147.6, 142.8, 139.2, 134.6, 132.5, 131.1, 130.9, 129.4, 129.3, 128.6, 126.0, 118.3, 21.2, 19.60, 14.4, 13.7 ; APCI-MS : *m/z* = 678 $[M]^+$ elemental analysis calculate (%) for $C_{34}H_{33}BF_2N_2Se_2$: C 60.36, H 4.92 N 4.14, found (%) :C 60.09, H 4.85, N 4.08

4,4'-Difluoro-1,3,5,7-tetramethyl-8- mesityl-2,6-di(selenophene-2-yl)-4-bora-3a,4a-diaza-*s*-indacene 2

To a solution of **4** (0.243 g, 0.393 mmol), 4,4,5,5-tetramethyl-2-(selenophen-2-yl)-1,3,2-dioxaborolane (0.253 g, 0.983 mmol), Pd(dppf)Cl_2 (0.1 g, 0.1 mmol) and a small amount of Aliquat 336 in deaerated toluene (25 mL), was added 2M K_2CO_3 aqueous solution (4 mL) under a N_2 atmosphere. The mixture was stirred at 90 °C for overnight. The resultant solution was poured into water and extracted with AcOEt. The organic phase was dried over Na_2SO_4 and filtrated. After removal solvent from the filtrate, the residue was chromatographed on silica gel (Wakogel C-300) using benzene / hexane (1:1 v/v) as an eluent to afford 0.132 g of **2** as red-green solid in 54% yield. ^{1}H NMR (500 MHz, $CDCl_3$) δ (ppm): 8.06 (2H, dd, J = 5.60 and 1.15 Hz), 7.31 (2H, dd, J = 5.65 Hz and 3.70 Hz), 7.02 (2H, dd, J = 3.65 and 1.05 Hz), 6.96 (2H, s), 2.61 (6H, s), 2.33 (3H, s), 2.16 (6H, s), 1.40 (6H, s). ^{13}C NMR (126 MHz, $CDCl_3$) δ (ppm): 154.5, 142.6, 140.1, 139.5, 138.9, 134.9, 131.8, 131.2, 130.4, 130.1, 129.7, 129.2, 128.2, 21.2, 19.7, 13.6, 11.8. FAB-MS: *m/z* = 626 $[M]^+$ Elemental analysis: Calcd. for $C_{30}H_{29}BF_2N_2Se_2$: C 57.72, H 4.68, N 4.49, found C 57.70, H 4.65, N 4.49.

The measurement of fluorescent quantum yield

The fluorescence quantum yields (Φ_F) were calculated from eq. (1).[48]

$$\Phi = \Phi_R \times \frac{\int_0^\infty F(\lambda)d\lambda}{\int_0^\infty F_R(\lambda)d\lambda} \times \frac{A_R}{A} \times \frac{n^2}{{n_R}^2} \quad (1)$$

Where $F(\lambda)$ and $F_R(\lambda)$ describe the corrected fluorescence intensities of the compound and the reference, respectively, and A and A_R describe the corresponding absorbance at the excitation wavelength. The reference

View Article Online
DOI: 10.1039/C8TC00944A

used was Rhodamine B (Φ_R = 97% in EtOH).[49]

X-ray crystallography for 1

A red prism crystal of **1** having approximate dimensions of 0.25 × 0.16 × 0.16 mm was mounted on a glass fiber. All measurements were made on a X-ray diffractometer using multi-layer mirror monochromated Mo-Kα radiation (λ = 0.71075 Å). The structure was solved by direct methods (SHELXS2013)[50] and expanded using Fourier techniques. The non-hydrogen atoms were refined anisotropically. Hydrogen atoms were refined using the riding model. The refinement was made by using a full-matrix least-squares technique (SHELXL2013).

Electrochemistry

Cyclic voltammograms (CV) were recorded on a potentiostat operated at a scan rate of 50 mV s^{-1} and room temperature under a N_2 atmosphere. The solvent was CH_2Cl_2 containing 0.1 M tetrabutylammonium hexafluorophosphate ($TBAPF_6$) as the supporting electrolyte. The potentials were measured against Ag/Ag^+ (0.01 M of $AgNO_3$) as a reference electrode; ferrocene/ferrocenium (Fc/Fc^+) was used as the internal standard and measured to be 0.22 V under same conditions. The onset potentials were determined from the intersection of two tangents drawn at the rising and background currents of the cyclic voltammogram.

Theoretical calculations

All geometries of the dyes at the ground state were fully optimized by means of the CAM B3LYP/6-31G(d,p) level method. Density functional theory (DFT) calculations at the CAM-B3LYP/6-31G(d,p) level were performed in the Gaussian 09 package.[51] (Gaussian 09, Gaussian, Inc, Wallingford, CT, 2010) These molecular orbitals were visualized using Gauss view 5.0.8 program. Based on the optimal structure time-dependent DFT (TD-DFT) with the PCM model was used to calculate the excitation energies of the lowest singlet S_1 and triplet T_1 states of sensitizers and annihilator.

Nanosecond transient absorption measurements

Transient absorption measurements were performed at ambient temperature using a monochromator (JASCO CT-25CP) and a photomultiplier (Hamamatsu Photonics R928) with continuous-wave illumination from a Xe lamp (JASCO PS-X150B).[52, 53] Time profiles of the photomultiplier signals were integrated using a digital oscilloscope (Iwatsu-LeCroy LT342). The time-profiles recorded point-by-point at 10 nm intervals were converted to absorbance values, and then the transient spectra were obtained using a personal computer. The samples were deaerated by freeze-pump-thaw cycles before the measurements, and were excited at 532 nm using an Nd:YAG laser (Spectra Physics INDI 40; 7 ns pulse width (FWHM)). The incident laser energy was attenuated to 0.3 mJ per pulse (transient absorption spectrum) or 0.01 mJ per pulse (time-profile at 450 nm).

Triplet-triplet annihilation upconversion

The upconversion fluorescence spectra were measured by a modified a JASCO FP-6500 spectrophotometer. A diode laser of 51 mW as maximum output power (RGB Lasersystems, 520 nm) was

View Article Online
DOI: 10.1039/C8TC00944A

used as the excitation light in the TTA-UC system. The diameter of the laser spot was 1.1×2.2 to 1.2×4.3 mm. The power of the laser beam was measured with a photopower meter (ADC, 8230E). The TTA-UC quantum yields (Φ_{UC}) were determined using the fluorescence of **I_2-BODIPY** as the standard (Φ_{ref} = 2.7% in MeCN),[34] the following equation being employed:

$\Phi_{UC} = \Phi_{ref}(A_{ref}/A_{UC})(I_{UC}/I_{ref})(\eta_{UC}/\eta_{ref})^2 = 0.5\Phi'_{UC}$

where Φ, A, I and η represent the quantum yield, absorbance, integrated fluorescence intensity and the refractive index of the solvent. The CIE coordinates of the UC emission were derived from spectra manager (FP6500 control driver). Although the maximum quantum yield (Φ_{UC}) of bimolecular TTA-UC process is 50%, related papers mostly adopt the value multiplied by 2 to set maximum quantum yield of 100%. In this study, we have used Φ'_{UC} ($2 \times \Phi_{UC}$).[16]

Results and Discussions

Synthesis and Characteristics of 1 and 2

Bis(phenylselanyl)-containing BODIPY **1** was synthesized through electrophilic substitution of **3** with phenylselanyl chloride in 85% yield after column chromatography (Scheme 1). To prepare selenophene-derivative **2**, starting material **3** was subjected to iodination, followed by a Suzuki reaction with 4,4,5,5-tetramethyl-2-(selenophen-2-yl)-1,3,2-dioxaborolane in the presence of Pd(dppf)Cl_2. The target selenium-containing BODIPYs **1** and **2** were fully assigned based on spectroscopic data.

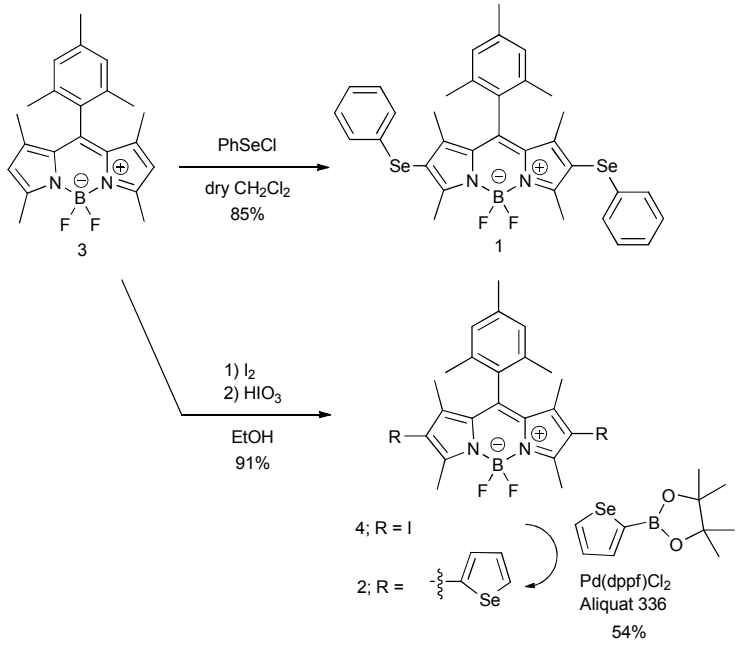

Scheme 1 Synthesis of selenium-containing BODIPY dyes **1** and **2**.

A red prism crystal of **1** was successfully obtained for X ray diffraction analysis. The structure belonged to the orthorhombic $P2_12_12_1$ group with four molecules in one unit cell (Fig. 2). As a typical feature, the phenylselenyl groups at the 2 and 6 positions of the BODIPY core were tilted by 65 ° and 73 ° with respect to the core structure,

View Article Online
DOI: 10.1039/C8TC00944A

as shown in Fig. 2b. Such torsion may be ascribed to intermolecular interactions in the packing structure (Fig. 2c). Indeed, CH-π interactions were observed between the phenylselanyl unit and mesityl group of the neighboring molecule.

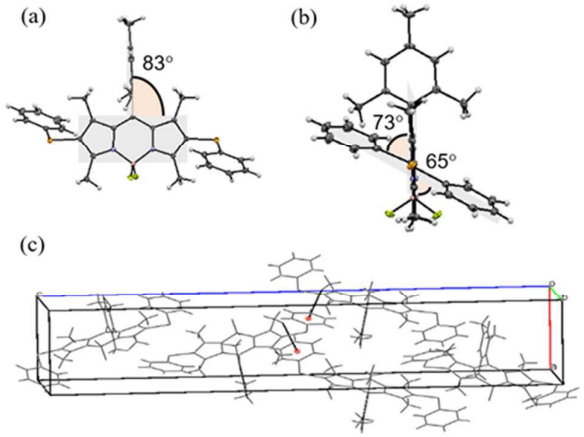

Fig. 2 X-ray crystal structure of **1** where thermal ellipsoids are drawn at the 50% probably level, showing front view (a), side view (b) and packing structure (c).

Fig. 3 shows absorption and fluorescence spectra of a series of BODIPYs in CH_2Cl_2 at 25 °C (data is summarized in Table S1). Selanyl-BODIPY **1** absorbs visible light at 518 nm, with a molar extinction coefficient (ε) of 7.84 × 10^4 M^{-1} cm^{-1}. Although the λ_{max} value is 16 nm larger than that of parent BODIPY **3**, a hypthochromic shift was observed as compared to iodide-appended BODIPY **4**. On another front, the λ_{max} value of selenophene derivative **2** was comparable to that of **4**, and **2** exhibited the lowest ε value among the tested dyes. The full width half maximum (FWHM) of **2** was 52 nm, whereas the FWHM of parent BODIPY **3** was 17 nm. Selenium-containing dyes **1** and **2** exhibited emission bands at 594 and 613 nm, respectively, and large Stokes shifts of about 2500 cm^{-1} as compared to **3** were observed. This suggested that the introduction of selenium-containing substituents at the 2 and 6 positions of the BODIPY core resulted in pronounced effects on the optical properties. Particularly, larger Stokes shift in **2** could be responsible for the remarkable geometry relaxation upon photoexcitation; notably, a similar behavior was observed in 2,6-bisthienyl BODIPY.[54] Further, the fluorescence quantum yield (Φ_F) of **1** was 0.03, being one-fifth as small as that of **2**. Such a low value may be attributed to the efficient ISC between the singlet and triplet state, which was comparable to that of **4** (Φ_F = 0.05). Considering the electron donor ability of selenium, we measured the solvent-dependency of the spectroscopic properties of **1** (Fig. S1 and Table S2). As solvent polarity increased, the Φ_F value decreased, and was accompanied by a shift in the emission to a longer wavelength, despite almost no change in the absorption band. This trend was rationalized by employing a Lippert-Mataga plot (Fig. S2),[55, 56] and the change in the static dipole moment of **1** ($\Delta\mu$) was calculated to be 11.2 D, indicating an intramolecular charge transfer (ICT) and a heavy atom effect due to selenium. As shown in Fig. S3 and Table S2, similar trend was observed in **2** with a relative small $\Delta\mu$ value (6.74 D; Fig. S4).

View Article Online
DOI: 10.1039/C8TC00944A

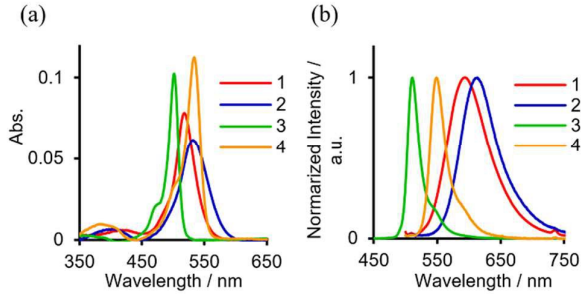

Fig. 3 Absorption (a) and fluorescence (b) spectra of dyes **1** − **4** (1.0 μM) in CH_2Cl_2.

The electrochemical properties of the dyes were investigated using cyclic voltammetry (CV). The formal potential of F_c/F_c^+ ($E_{1/2}^{Fc/Fc+}$) was 0.220 V *versus* Ag/Ag^+. Reversible reduction waves were observed with half-wave potentials ($E_{1/2}^{red}$) of −1.24 V for **1** and −1.41 V for **2**, respectively (Fig. 4). Given that the $E_{1/2}^{red}$ of **3** was −1.55V, selenium incorporation onto BODIPY led to the stabilization of the LUMO energy level. On the other hand, a reversible oxidation wave was observed for **1** with an $E_{1/2}^{ox}$ of 1.01 V. When the measurements were calibrated against ferrocene (−4.8 eV) as the standard,[57] the HOMO energy level of **1** was estimated to be −5.59 eV. Taking into account the LUMO energy level (−3.24 eV), which was estimated from the $E_{1/2}^{red}$ value, the electrochemical band gap was 2.35 eV (527 nm), which was almost similar to that of the experimental value (Fig. 3). In contrast, **2** showed an irreversible oxidation wave with an E_{pa} of 0.96 V. The HOMO and LUMO of **2** were higher than those of **1**, possibly due to the electron donor ability of the selenophene moiety.

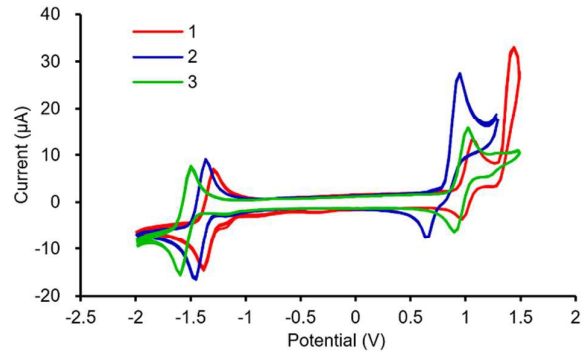

Fig. 4 Cyclic voltammetry of **1** − **3** in CH_2Cl_2 solution containing 0.1 M $TBAPF_6$. The scan rate is 0.05 V s^{-1}.

To obtain further insight into the triplet excited state of the sensitizers, time-resolved fluorescence measurements were carried out (Fig. S5). The fluorescence lifetime (τ_F) of **1** was determined to be 0.285 ns in CH_2Cl_2, which was significantly shorter than that of **2** (1.84 ns). The $^1O_2$ production quantum yields (Φ_Δ) of the dyes were also evaluated using 1,3-diphenyisobenzofuran (DPBF), a well-known singlet oxygen indicator.[58] As shown in Fig. S6, the absorption intensity of DPBF in CH_2Cl_2 decreased with time, due to photooxygenation. Notably, **1** showed a high Φ_Δ of 0.86, which was almost similar to that of **I_2-BODIPY**. Moreover, the Φ_Δ value of **2** was one-third that of **1**. Assuming that the energy transfer efficiency could be 100% from the excited T_1 state of the dye to $^3O_2$, $\Phi_\Delta = \Phi_{ISC}$ (quantum yield of intersystem crossing). Combined with the fluorescence lifetime and Φ_{ISC} values, the relevant parameters of the photophysical process were obtained using the following equations, eqs. (1) – (3):

View Article Online
DOI: 10.1039/C8TC00944A

$$\tau_F = \frac{1}{k_F + k_{IC} + k_{ISC}} \quad (1)$$

$$\Phi_F = \frac{k_F}{k_F + k_{IC} + k_{ISC}} \quad (2)$$

$$\Phi_{ISC} = \Phi_\Delta = \frac{k_{ISC}}{k_F + k_{IC} + k_{ISC}} \quad (3)$$

where k_F, k_{IC} and k_{ISC} are the rate of fluorescence, internal conversion, and intersystem crossing, respectively. k_F, k_{IC} and k_{ISC} are summarized in Table 1. The k_{ISC} value of **1** was calculated to be 3.02×10^9 s^{-1}, which was 19 times larger than that of **2**, indicating that the singlet excited state of **1** was effectively converted into the corresponding triplet state. Furthermore, the phosphorescence spectra of **1** and **2** were measured at 77 K; peaks at 746 and 756 nm were observed in toluene for **1** and **2**, respectively (Fig. S7).[59] The ΔE_{ST} (= $E_S - E_T$) was calculated to be 0.43 for **1** and 0.38 eV for **2**. The slight difference in ΔE_{ST} values indicates that the heavy atom effect of selenium affected Φ_{ISC}.

Table 1. Photophysical properties of dyes **1** and **2** in CH_2Cl_2 at 25 °C.

Dye	λ_{abs} / nm	ε / 10^4 M^{-1} cm^{-1}	λ_F /nm[a]	Φ_F	τ_F /ns[b]	Φ_Δ[d] = Φ_{ISC}	k_F / ns^{-1}	k_{IC} / ns^{-1}	k_{ISC} / ns^{-1}	λ_p /nm[c]
1	518	7.84	594	0.03	0.285	0.86	0.105	0.386	3.02	746
2	532	6.15	613	0.16	1.84	0.30	0.0978	0.282	0.163	756

[a]The excitation wavelengths of **1** and **2** were 490 nm, respectively. [b]Singlet state lifetime, excited at 405 nm for **1** and 590 nm for **2**, respectively. [c]Phosphorescence maxima in toluene at 77 K, excited at 540 nm for **1** and **2**, respectively. [d]Singlet oxygen quantum yield.

A better understanding of the photophysical properties of **1** allowed us to carry out density functional theory (DFT) and time-dependent density functional theory (TD-DFT) analysis at the CAM-B3LYP/6-31G(d,p) level.[60] Structural optimizations revealed that the dihedral angles between phenylselanyl plane and BODIPY core were 63 ° and 71 °. The calculated absorption bands were located at 435 and 349 nm, and were assigned to the $S_0 \rightarrow S_1$ and $S_0 \rightarrow S_2$ transitions, respectively. Based on the oscillator strength, the main transition was assigned to the $S_0 \rightarrow S_1$ transition where the HOMO → LUMO was the major configuration of the transition. The electron-density distribution in the HOMO was spread over the BODIPY core and selanyl moieties, whereas the corresponding surface plot of the LUMO spread over the BODIPY core. This represents a $\pi-\pi^*$ transition involving the ICT from the phenylselanyl moiety to the BODIPY core, which was supported by the solvent polarity-dependent photophysical properties. On another front, the $S_0 \rightarrow S_2$ transition was assigned to the broad absorption band at 418 nm ($\varepsilon = 5.91\times10^3$ M^{-1} cm^{-1}), as shown in Fig. 3 (*vide supra*). The T_1 state of **1** was optimized where the orientation of the phenylselanyl moieties was similar to that in the S_0 state. The vertical $S_0 \rightarrow T_1$ excitation was calculated by the DFT/TD-DFT method. The molecular orbitals in the transition was shown in Fig. 5. The T_1 state

View Article Online
DOI: 10.1039/C8TC00944A

is localized on the BODIPY core and does not have CT character. Fig. 5 also shows the spin density surface at the optimized triplet geometry, indicating that the T_1 state was located on the BODIPY core. Such localization strongly supports that the direct introduction of selenium onto the BODIPY core should be effective for the production of the T_1 state through an efficient ISC path. To verify the production of the triplet state upon photoexcitation, nanosecond transient absorption measurements were carried out upon pulsed excitation at 532 nm. For the measurements, molecular oxygen dissolved in the solution was carefully removed by freeze-pump-thaw cycles. And the pulsed laser energy was low enough to avoid T−T annihilation. As shown in Fig. 6a, a broad transition absorption band at ca 450 nm was observed, being attributable to absorption of the T_1 state of **1**. The decay profile at 450 nm allowed us to determine the lifetime (τ) of 1.4 ms. The T_1 energy was evaluated to be 1.66 eV from the phosphorescence spectrum. We reasoned that triplet-triplet energy transfer (TTET) between these dyes and perylene (1.53 eV)[44] would be thermodynamically possible.

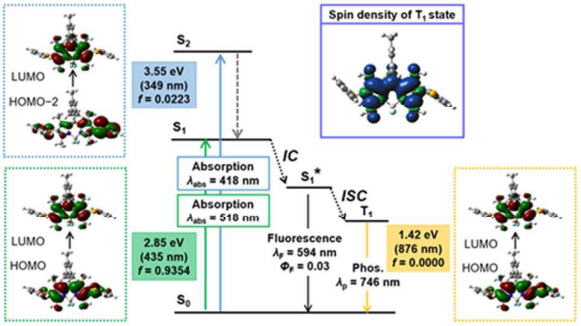

Fig. 5 A simplified Jablonski diagram illustrating the photophysical properties of **1** in CH_2Cl_2 where selected frontier orbitals in the singlet and triplet excited states are described. The excitations were calculated by DFT/TD-DFT at the CAM-B3LYP/6-31G (d,p) level with Gaussian 09W. Phosphorescence spectrum was measured at 77 K in toluene. IC and ISC denote internal conversion and intersystem crossing, respectively.

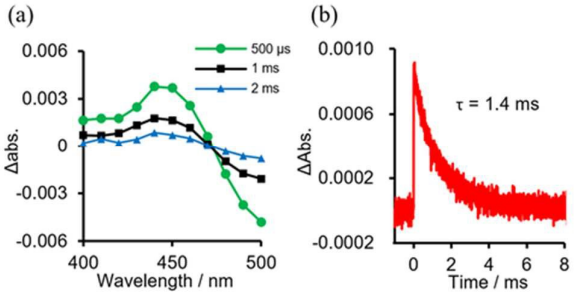

Fig. 6. (a) Nanosecond transient absorption spectra of **1** (10 μM) in deaerated toluene. (b) Decay profile of the transient at 450 nm of **1** at room temperature.

TTA-UC study in solution

We investigated the TTA-UC process of **1** (10 μM) and perylene as an annihilator in deaerated toluene upon photo-excitation with a 524 nm laser (5 mW). Upconverted emission with λ_{em} values of 449 and 473 nm indicated a significant anti-Stokes shift of 75 nm in the UC process, which was consistent with the fluorescence spectrum of perylene (Fig. 7a). The longer emission at 591 nm was ascribed to the fluorescence of **1**. To explore the optimal conditions for UC behavior, upconverted emissions were measured by varying concentration of perylene. Fig. 7b

View Article Online
DOI: 10.1039/C8TC00944A

shows the relationship of Φ'_{UC} *vs.* perylene concentration; the curve almost leveled off when more than 20 μM perylene was added.[61] As a result, the bi-molecular system of **1** (10 μM) and perylene (30 μM) provided an efficient Φ'_{UC} of 12% in deaerated toluene under excitation with a 524 nm laser (5.0 mW). Compared to the Φ'_{UC} of 0.5% for the related system comprised of **2** and perylene (Fig. S8), the direct connection of selenium heavy atom into BODIPY core was more effective for the upconverted behavior. Although dye **1** emitted orange light under irradiation at 532 nm (100 mW cm^{-2}), the addition of perylene to the solution resulted in purplish white light (Fig. 8), which deviated marginally from the ideal white light (0.33, 0.33) of the CIE chromaticity coordinates. To determine if this behavior originated from the TTA-UC mechanism, we measured the excitation power-dependency on the upconverted emission in deaerated toluene. A linear relationship was obtained from the double-logarithm plot of the UC emission intensity as a function of incident power density at 524 nm (Fig. 9).[3, 62, 63] A slope of 1.95 was obtained at a lower power range, and a slope of 1.11 was obtained at a higher power density (≥ 116 mW cm^{-2}). As a result, the crossing point of the two fitting lines gave an excitation power threshold (I_{th})[64, 65] of 116 mW cm^{-2}, which represented the main parameter for the TTA-based upconversion process at which half of the triplet sensitizer was subjected to TTA. The intermolecular TTET process between the triplet excited states of **1** and perylene is among the key parameters for TTA-UC, and was investigated by quenching titrations of the phosphorescence of **1** upon adding increasing amounts of perylene (Fig. S9). Although the phosphorescence intensity was decreased upon addition of perylene, our attempt to determine the Stern-Volmer constant was unsuccessful because of the low intensity. It has been reported that the Φ_p values of halogenated BODIPYs are in the order of 10^{-3}.[66]

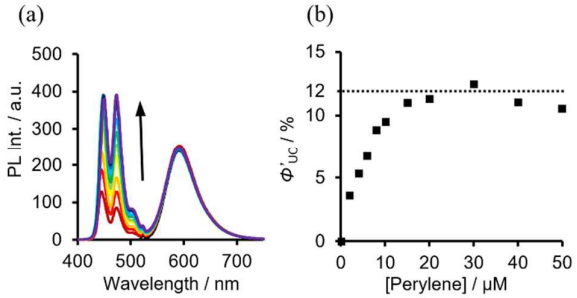

Fig. 7 (a) Change in upconverted fluorescence upon addition of different amounts of perylene in deaerated toluene. (b) Φ'_{UC} value as a function of perylene concentration in deaerated toluene. Excited with a 524 nm laser (5 mW). [**1**] = 10 μM.

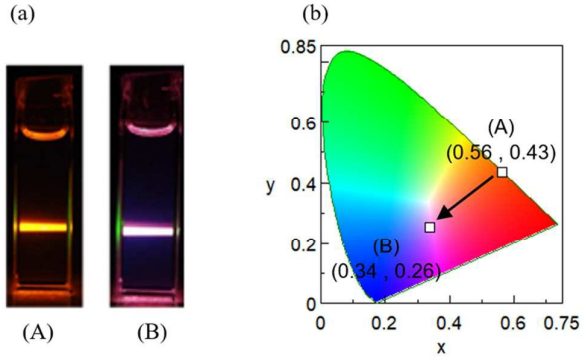

Fig. 8 (a) Images of fluorescence of **1** (10 μM) (A) and **1** (10 μM) plus perylene (30 μM) (B). (b) CIE chromaticity coordinates for the emission behaviors of (A) and (B). λ_{ex} = 532 nm (100 mW cm^{-2}).

View Article Online
DOI: 10.1039/C8TC00944A

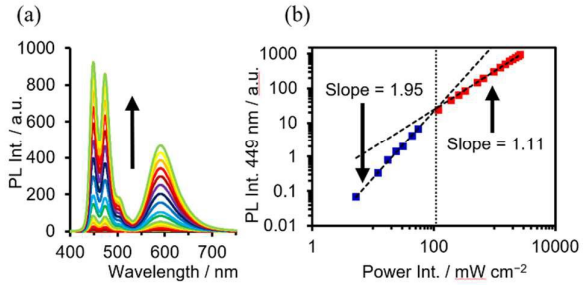

Fig. 9 Excitation power dependency of upconverted perylene emission with **1** as a sensitizer. (a) Photoluminescence spectra. (b) UC emission intensity at 449 nm at different power intensities. [**1**] = 10 μM, [perylene] = 30 μM in degassed toluene upon irradiation with a 524 nm laser (5.24 ~ 2650 mW cm^{-2}).

Considering the ICT characteristics of dye **1**, we measured the UC behavior in deaerated CH_2Cl_2 (Fig. S10); a Φ'_{UC} of 17% was obtained, which was larger than that in deaerated toluene. As a control experiment, a bi-molecular system composed of **I_2-BODIPY** (10 μM) and perylene (30 μM) was investigated under similar conditions (Fig. S11). A Φ'_{UC} of 16% was obtained, which was similar to that of **1** and perylene in deaerated CH_2Cl_2. In addition, the ICT of sensitizer **1** enabled us to tune the emission color of the UC system by varying the solvent. Upon replacing toluene with CH_2Cl_2, a purplish white emission corresponding to CIE coordinate (0.34, 0.26) changed to that of (0.25, 0.18) (Fig. S12). Such solvent dependency on the upconversion efficiency may be due to the triplet-state generation efficiency of **1**.

Conclusion

In this work, selenium-containing BODIPY dyes **1** and **2** were synthesized as photosensitizers for TTA-UC systems. The introduction of a phenylselanide group at the 2 and 6 positions of the BODIPY core endowed the dye with ICT characteristics. Although electron-donor strength of selenophene unit in **2** is larger than that of phenylselanyl unit in **1**, the direct binding of selenium to the pyrrole carbon led to a heavy atom effect on the photophysical properties. Significant upconverted fluorescence by perylene was observed with dye **1** upon excitation with a 524 nm laser (5.0 mW). Subsequently, a significant anti-Stokes shift of 77 nm with a Φ'_{UC} value of 17% was observed in CH_2Cl_2; the quantum yield was comparable to that of **I_2-BODIPY**. Due to the π−π* transition involving the ICT of **1**, the emission color of the solution, arising from the fluorescence of sensitizer **1**, and the upconverted emission of perylene could be tuned by the solvent polarity. The excited state of **1** was rationalized by time-resolved fluorescence spectroscopic analysis, phosphorescence measurements, $^1O_2$ detection and nanosecond transient absorption spectroscopy. The simple and straightforward synthesis of selenium-containing π-conjugated systems would be useful for the preparation of photosensitizers applicable to NIR upconversion, which deserves further investigation.

Acknowledgments

This research was supported by The Iwatani Naoji Foundation's research grant and JSPS KAKENHI Grant Numbers 26620033 and 17H06375.

Notes and references

1. T. N. Singh-Rachford and F. N. Castellano, *Coord. Chem. Rev.*, 2010, **254**, 2560-2573.

View Article Online
DOI: 10.1039/C8TC00944A

2. F. Wang and X. Liu, *Chem. Soc. Rev.*, 2009, **38**, 976-989.
3. J. Zhou, Q. Liu, W. Feng, Y. Sun and F. Li, *Chem. Rev.*, 2015, **115**, 395-465.
4. X. Zhu, Q. Su, W. Feng and F. Li, *Chem. Soc. Rev.*, 2017, **46**, 1025-1039.
5. N. Yanai and N. Kimizuka, *Chem. Commun.*, 2016, **52**, 5354-5370.
6. Y. C. Simon and C. Weder, *J. Mater. Chem.*, 2012, **22**, 20817-20830.
7. A. Monguzzi, S. M. Borisov, J. Pedrini, I. Klimant, M. Salvalaggio, P. Biagini, F. Melchiorre, C. Lelii and F. Meinardi, *Adv. Funct. Mater.*, 2015, **25**, 5617-5624.
8. V. Gray, D. Dzebo, M. Abrahamsson, B. Albinsson and K. Moth-Poulsen, *Phys. Chem. Chem. Phys.*, 2014, **16**, 10345-10352.
9. S. H. C. Askes, W. Pomp, S. L. Hopkins, A. Kros, S. Wu, T. Schmidt and S. Bonnet, *Small*, 2016, **12**, 5579-5590.
10. S. Mattiello, A. Monguzzi, J. Pedrini, M. Sassi, C. Villa, Y. Torrente, R. Marotta, F. Meinardi and L. Beverina, *Adv. Funct. Mater.*, 2016, **26**, 8447-8454.
11. Q. Dou, L. Jiang, D. Kai, C. Owh and X. J. Loh, *Drug Discovery Today*, 2017, **22**, 1400-1411.
12. J. Zhao, W. Wu, J. Sun and S. Guo, *Chem. Soc. Rev.*, 2013, **42**, 5323-5351.
13. Z. Wang and J. Zhao, *Org. Lett.*, 2017, **19**, 4492-4495.
14. K. Chen, W. Yang, Z. Wang, A. Iagatti, L. Bussotti, P. Foggi, W. Ji, J. Zhao and M. Di Donato, *J. Phys. Chem. A*, 2017, **121**, 7550-7564.
15. Z. Wang, J. Zhao, A. Barbon, A. Toffoletti, Y. Liu, Y. An, L. Xu, A. Karatay, H. G. Yaglioglu, E. A. Yildiz and M. Hayvali, *J. Am. Chem. Soc.*, 2017, **139**, 7831-7842.
16. D. Wei, F. Ni, Z. Zhu, Y. Zou and C. Yang, *J. Mater. Chem. C*, 2017, **5**, 12674-12677.
17. A. Loudet and K. Burgess, *Chem. Rev.*, 2007, **107**, 4891-4932.
18. G. Ulrich, R. Ziessel and A. Harriman, *Angew. Chem. Int. Ed.*, 2008, **47**, 1184-1201.
19. N. Boens, B. Verbelen and W. Dehaen, *Eur. J. Org. Chem.*, 2015, **2015**, 6577-6595.
20. S. G. Awuah and Y. You, *RSC Advances*, 2012, **2**, 11169-11183.
21. A. Kamkaew, S. H. Lim, H. B. Lee, L. V. Kiew, L. Y. Chung and K. Burgess, *Chem. Soc. Rev.*, 2013, **42**, 77-88.
22. L. Yao, S. Xiao and F. Dan, *Journal of Chemistry*, 2013, **2013**, Article ID 697850.
23. A. Bessette and G. S. Hanan, *Chem. Soc. Rev.*, 2014, **43**, 3342-3405.
24. Y. Ni and J. Wu, *Organic & Biomolecular Chemistry*, 2014, **12**, 3774-3791.
25. K. Umezawa, D. Citterio and K. Suzuki, *Anal. Sci.*, 2014, **30**, 327-349.
26. B. J. Müller, S. M. Borisov and I. Klimant, *Adv. Funct. Mater.*, 2016, **26**, 7697-7707.
27. A. Zampetti, A. Minotto, B. M. Squeo, V. G. Gregoriou, S. Allard, U. Scherf, C. L. Chochos and F. Cacialli, *Sci. Rep.*, 2017, **7**, 1611.
28. O. Suryani, Y. Higashino, J. Y. Mulyana, M. Kaneko, T. Hoshi, K. Shigaki and Y. Kubo, *Chem. Commun.*, 2017, **53**, 6784-6787.
29. S. Erten-Ela, Y. Ueno, T. Asaba and Y. Kubo, *New J. Chem.*, 2017, **41**, 10367-10375.
30. Y. Kubo, S. Tobinaga, Y. Ueno, T. Aotake, H. Yakushiji and T. Yamamoto, *Chem. Lett.*, 2018, **47**, 300-303.

View Article Online
DOI: 10.1039/C8TC00944A

31. J. Zhao, K. Xu, W. Yang, Z. Wang and F. Zhong, *Chem. Soc. Rev.*, 2015, **44**, 8904-8939.
32. X. Cui, A. Charaf-Eddin, J. Wang, B. Le Guennic, J. Zhao and D. Jacquemin, *J. Org. Chem.*, 2014, **79**, 2038-2048.
33. C. Zhang and J. Zhao, *J. Mater. Chem. C*, 2016, **4**, 1623-1632.
34. W. Wu, H. Guo, W. Wu, S. Ji and J. Zhao, *J. Org. Chem.*, 2011, **76**, 7056-7064.
35. Q. Zhou, M. Zhou, Y. Wei, X. Zhou, S. Liu, S. Zhang and B. Zhang, *Phys. Chem. Chem. Phys.*, 2017, **19**, 1516-1525.
36. X. Cui, A. M. El-Zohry, Z. Wang, J. Zhao and O. F. Mohammed, *J. Phys. Chem, C*, 2017, **121**, 16182-16192.
37. T. Yogo, Y. Urano, Y. Ishitsuka, F. Maniwa and T. Nagano, *J. Am. Chem. Soc.*, 2005, **127**, 12162-12163.
38. S. Santoro, J. B. Azeredo, V. Nascimento, L. Sancineto, A. L. Braga and C. Santi, *RSC Adv.*, 2014, **4**, 31521-31535.
39. C. W. Nogueira, G. Zeni and J. B. T. Rocha, *Chem. Rev.*, 2004, **104**, 6255-6286.
40. S. T. Manjare, Y. Kim and D. G. Churchill, *Acc. Chem. Res.*, 2014, **47**, 2985-2998.
41. S. Panda, A. Panda and S. S. Zade, *Coord. Chem. Rev.*, 2015, **300**, 86-100.
42. F. Yu, P. Li, G. Li, G. Zhao, T. Chu and K. Han, *J. Am. Chem. Soc.*, 2011, **133**, 11030-11033.
43. Z. Lou, P. Li and K. Han, *Acc. Chem. Res.*, 2015, **48**, 1358-1368.
44. T. N. Singh-Rachford and F. N. Castellano, *J. Phys. Chem. Lett.*, 2010, **1**, 195-200.
45. A. B. Nepomnyashchii, M. Bröring, J. Ahrens and A. J. Bard, *J. Am. Chem. Soc.*, 2011, **133**, 8633-8645.
46. R. P. Sabatini, B. Lindley, T. M. McCormick, T. Lazarides, W. W. Brennessel, D. W. McCamant and R. Eisenberg, *J. Phys. Chem. B*, 2016, **120**, 527-534.
47. S. Haid, A. Mishra, C. Uhrich, M. Pfeiffer and P. Bäuerle, *Chem. Mater.*, 2011, **23**, 4435-4444.
48. G. A. Crosby and J. N. Demas, *J. Phys. Chem.*, 1971, **75**, 991-1024.
49. G. Weber and F. W. J. Teale, *Trans. Faraday Soc.*, 1957, **53**, 646-655.
50. G. M. Sheldrick, *Acta Cryst. C*, 2008, **64**, 112-122.
51. M. J. Frisch, G. W. Trucks, H. B. Schlegel, G. E. Scuseria, M. A. Robb, J. R. Cheeseman, G. Scalmani, V. Barone, B. Mennucci, G. A. Petersson, H. Nakatsuji, M. L. Caricato, X., H. P. Hratchian, A. F. Izmaylov, J. Bloino, G. Zheng, J. L. Sonnenberg, M. Hada, M. Ehara, K. Toyota, R. Fukuda, J. Hasegawa, M. Ishida, T. Nakajima, Y. Honda, O. Kitao, H. Nakai, T. Vreven, J. A. Montgomery, Jr., J. E. Peralta, F. Ogliaro, M. Bearpark, J. J. Heyd, E. Brothers, K. N. Kudin, V. N. Staroverov, T. Keith, R. Kobayashi, J. Normand, K. Raghavachari, A. Rendell, J. C. Burant, S. S. Iyengar, J. Tomasi, M. Cossi, N. Rega, J. M. Millam, M. Klene, J. E. Knox, J. B. Cross, V. Bakken, C. Adamo, J. Jaramillo, R. Gomperts, R. E. Stratmann, O. Yazyev, A. J. Austin, R. Cammi, C. Pomelli, J. W. Ochterski, R. L. Martin, K. Morokuma, V. G. Zakrzewski, G. A. S. Voth, P., J. J. Dannenberg, S. Dapprich, A. D. Daniels, O. Farkas, J. B. Foresman, J. V. Ortiz, J. Cioslowski and D. J. Fox, Gaussian 09, Gaussian, Inc, Wallingford, CT, **2010**.
52. K. Ishii, Y. Hirose, H. Fujitsuka, O. Ito and N. Kobayashi, *J. Am. Chem. Soc.*, 2001, **123**, 702-708.
53. K. Ishii, S. Takeuchi, S. Shimizu and N. Kobayashi, *J. Am. Chem. Soc.*, 2004, **126**, 2082-2088.
54. Y. Chen, J. Zhao, H. Guo and L. Xie, *J. Org. Chem.*, 2012, **77**, 2192-2206.
55. V. E. Z. Lippert, *Elektrochem.*, 1957, **61**, 962-975.

View Article Online
DOI: 10.1039/C8TC00944A

56. N. Mataga, Y. Kaifu and M. Koizumi, *Bull. Chem. Soc. Jpn.*, 1956, **29**, 465-470.
57. J. Pommerehne, H. Vestweber, W. Guss, R. F. Mahrt, H. Bässler, M. Porsch and J. Daub, *Adv. Mater.*, 1995, **7**, 551-554.
58. E. A. Lissi, M. V. Encinas, E. Lemp and M. A. Rubio, *Chem. Rev.*, 1993, **93**, 699-723.
59. No phosphorescence spectrum was observed for parent BODIPY **3** in toluene at 77 K. λ_{ex} = 490 nm.
60. Z.-L. Cai, M. J. Crossley, J. R. Reimers, R. Kobayashi and R. D. Amos, *J. Phys. Chem. B*, 2006, **110**, 15624-15632.
61. With excess perylene, the slight decrease in Φ'UP may be due to self-absorption by perylene.
62. P. Duan, N. Yanai and N. Kimizuka, *J. Am. Chem. Soc.*, 2013, **135**, 19056-19059.
63. P. Duan, N. Yanai, H. Nagatomi and N. Kimizuka, *J. Am. Chem. Soc.*, 2015, **137**, 1887-1894.
64. A. Monguzzi, J. Mezyk, F. Scotognella, R. Tubino and F. Meinardi, *Phys. Rev. B*, 2008, **78**, 195112.
65. A. Monguzzi, J. Mezyk, F. Scotognella, R. Tubino and F. Meinardi, *Phys. Rev. B*, 2009, **80**, 039904.
66. X.-F. Zhang, X. Yang, K. Niu and H. Geng, *J. Photochem. Photobiol., A.*, 2014, **285**, 16-20.

View Article Online
DOI: 10.1039/C8TC00944A

New 2,6-bis(phenylselanyl)-BODIPY **1** was synthesized and served as a triplet photosensitizer for triplet-triplet annihilation upconversion (TTA-UC).